INVESTIGATION OF MACHINING BEHAVIOUR OF FLAX REINFORCED EPOXY COMPOSITES USING THE ANN APPROACH

MANIKANDAPRABU NALLASIVAM,[*] SHETTAHALLI MANTAIAH VINU KUMAR,[**] CHANDRASEKARAN SASIKUMAR[***] and RISHI JAYAPRAKASH[****]

[*]*Department of Electronics and Communication Engineering, Sri Krishna College of Engineering and Technology, Kuniyamuthur, Coimbatore, Tamil Nadu, India*
[**]*Department of Mechanical Engineering, Sri Krishna College of Engineering and Technology, Kuniyamuthur, Coimbatore, Tamil Nadu, India*
[***]*Department of Mechanical Engineering, Bannari Amman Institute of Technology, Sathyamangalam, Tamil Nadu, India*
[****]*Department of Mechanical Engineering, Vidyavardhaka College of Engineering Mysuru, Karnataka, India*
✉ *Corresponding author: S. M. Vinu Kumar, vinukmr1988@gmail.com*

Received April 29, 2025

In this study, flax fiber reinforced epoxy (FFRE) composites were fabricated using the hand layup method. The effects of spindle speed (900, 1800, 2700 rpm), feed rate (70, 90, 110 mm/min), and end mill cutters (6, 8, 10 mm) on milling behavior were analyzed. Milling tests were conducted on a vertical CNC machine for a 2 mm constant depth of cut. Experimental details followed Taguchi's L_{27} orthogonal array, where cutting force and surface roughness (R_a) were evaluated as output responses. The investigation revealed that cutting force increased with the increase in the feed rate, but decreased as spindle speed was increased. Better surface quality of the milled surface in terms lower cutting force and surface roughness value was achieved at the optimal input conditions. Artificial neural network (ANN) models with different architectures were implemented to predict the cutting force and surface roughness. The analysis showed that predicted values were in close agreement with the experimental results and exhibited a maximum error deviation of ±5%, particularly when 3-5-4-1, and 3-5-4-2 ANN models (Purelin-Purelin-Purelin Transfer function) were employed for single and dual output respectively. The accuracy of the aforesaid models was measured in terms of highest R^2 value and lowest mean absolute percentage error (MAPE). Field emission scanning electron microscopy (FESEM) images of the machined surface exposed matrix damage, cavity formation, fiber pull-out, and micro-tear.

Keywords: flax-epoxy composites, milling, ANN, surface roughness, cutting force, FESEM

INTRODUCTION

In recent times, consistent research efforts have been made to develop recyclable and environmentally sustainable composite materials.[1] To curb down greenhouse gas emissions, interest in producing environmentally friendly, renewable materials is the highest priority. Therefore, the production of natural fiber reinforced composites (NFRC) for various application areas, has been significantly increased.[2] In the automotive sector, it is estimated that, by the end of 2050, 50% of the reinforcement material in the polymer composite will be from plant based and renewable sources.[3] Plant fibers are widely available in the nature and have a comparatively lower cost than animal and man-made fibers. Their mechanical properties are, however, lower than those of synthetic fibers. Still, owing to their biodegradability and sustainability characteristics, they are a subject of much interest.[4] Flax, jute, sisal, hemp, kenaf and bamboo fibers are amongst the natural fibers that are widely used as reinforcement material in preparing NFRCs.[5]

Initially, NFRC usage was limited to home appliances, but, considering environment and industrial demands, research on NFRCs has expanded, focusing on their properties and potential applications. Many investigations have been reported on the mechanical, thermal, and dynamic mechanical properties of natural fiber composites. The effects of fiber orientation, fiber types, fiber architecture, weight fraction of fiber, hybridization, stacking sequence, processing method, chemical treatment, matrix type, manufacturing parameters *etc*., on the properties of NFRCs have been extensively studied.[4,6,7]

In order to accomplish a full scale product manufactured from composite parts, additional secondary processing operations are required.[8] Therefore, understanding the machinability properties of composites is as important as knowing their physico-mechanical, thermal and wear properties. In most applications, composites are joined using temporary mechanical fasteners. The stability and integrity of the assembly mainly relies on the quality of the drilled holes, which need to be free from delamination, and other surface defects. Therefore, the drilling behavior of NFRCs is of interest, with a special focus on how to improve the quality of drilled holes by reducing the delamination factor, considering all the input factors, such as drill diameter, drill type, feed rate, and spindle speed. In this context, Kumar *et al.*[9] studied the free vibration and drilling behavior of flax-epoxy composites using the ANFIS technique. Experimental results showed that high spindle speed with minimum feed significantly affected the thrust force generated in the composites. ANFIS prediction was found to be highly effective in forecasting the thrust force, compared to the response surface method. Raja *et al.*[10] optimized the drilling parameters in sisal–human hair hybrid composite using GRA. They observed that feed rate affects the delamination of the hybrid composite at the entry side of the hole, whereas the drill point angle – on the exit side. Valarmathi *et al.*[11] predicted the surface roughness quality of the drilled hole in particleboard composites using RSM and ANFIS, and the latter method was found to be more effective than the former one. Similar findings were reported by Vinu Kumar *et al*.,[12] namely, that torque response in drilling jute-epoxy composites is highly affected by feed rate, followed by spindle speed and drill point angle. ANFIS was found to be highly accurate in forecasting the torque with R^2 value of 0.9982. Jayabal *et al.*[13] concluded in their study that machinability of the glass and coconut fiber reinforced hybrid composite highly depends on the feed rate.

Milling is another important machining process employed in NFRCs, mainly used for plate parts. However, fiber pullouts, micro-tear, fiber breakage, matrix softening, delamination and tool wear are prime defects to be considered while milling NFRCs, as they may affect the quality of the milled surface and may then affect the fitting tolerance when composite components are assembled. Thus, finding the optimum milling parameters to reduce those aforesaid defects is essential. However, few studies have been reported on the milling behaviour of NFRCs. For example, Celik *et al.*[14] studied the milling of jute fiber reinforced polymer composites using cemented carbide end mills. They proposed that the cutting force produced during milling and the surface roughness value of the composite were highly influenced by spindle speed and feed rate.[22] Thus, an end mill cutter with higher flutes operated at higher spindle speed, with a lower feed rate, may produce a smoother surface. Vinayagamoorthy and Rajeswari[15] studied milling of jute-isophthalic polyester composites. The output responses, *i.e.* thrust force and torque, were highly affected by the input parameters: cutting speed, feed rate and depth of cut. Babu *et al.*[16] found that major issues, such as delamination of layers, and surface roughness in the milled hemp, jute and banana leaf reinforced polymer composites were mainly associated with cutting parameters and material composition. Kumar *et al.*[17] studied the effect of fiber orientation on milling glass fiber reinforced polymer composites. Experimental results revealed that fiber orientation influenced the cutting force and had less effect on cutting parameters. However, the machinability index was highly affected by feed rate. Chegdnai *et al.*[18] examined the tool wear mechanism in milling NFRCs. Slamani *et al.*[19] concluded that feed rate has a predominant effect on cutting forces and surface roughness in milling flax-epoxy composites, which was also confirmed by other researhers.[23] However, fiber orientation had less impact on the output responses. Though cutting speed was found to be less effective, it remains significant. Ragunath *et al.*[20] developed nanoclay reinforced natural/glass fiber hybrid polymer composites and studied the effects of different input factors on their milling responses. They observed that feed rate was the most significant factor, followed by other factors, such as nanoclay content, depth of cut and spindle speed. Higher nanoclay addition decreased the surface roughness value of the hybrid composites. Prasanthi *et al.*[21] reported the effect of fiber orientation on the milling behaviour of natural bagasse fiber reinforced polymer composites. Their results showed that machining 0° fiber oriented composites was more challenging than machining 45° fiber-oriented composites. Also, later composites required lower cutting force and thus higher surface quality could be achieved during milling. Moreover, it imparts stable machining operation.

From the literature survey presented above, it is noted that little research has been reported particularly on milling of NFRCs. Therefore, the present study explores the effect of cutting parameters on cutting force and surface roughness in milling of FFRE composites. Artificial neural

networks have been employed to predict the output responses, which were trained using the back propagation technique. This technique is widely employed by researchers as its prediction efficiency is higher than that of any other statistical tool and could forecast the performance of the system well before testing. Furthermore, FESEM analysis of the milled surface of the composites was carried out to observe the surface damages endured by the composites during the machining process.

EXPERIMENTAL

Materials

In this investigation, epoxy resin was selected as a matrix material, it was supplied by Vasavibala Resins, Chennai (India). Flax woven fabric was prepared from 6LEA yarn, procured from local vendors, Erode (India). A tabletop hand loom machine (ERGO G2) was utilized to make the flax fabric of irregular basket woven structure (BIT-Sathy), as shown in Figure 1 (areal density = 578 g/m^2). For carrying out the milling operation, an HSS end mill cutter of various sizes, supplied by Orient Hardware & Tools Corporation, Coimbatore, India, was employed.

Fabrication of flax fiber reinforced epoxy composite

The fabrication of FFRE composite was accomplished by the hand layup process, followed by curing of stacked laminates in a compression moulding machine under controlled pressure and room temperature. Initially, a known weight of the woven flax fiber was measured for preparing 40 wt% of FFRE composites. The epoxy and hardener blend was prepared by mixing at a proper ratio, as prescribed by the producer. The first layer of flax woven fabric was laid on the steel mould (250 mm × 250 mm × 4 mm), over which the epoxy-hardener blend was applied using a brush, the resin was spread evenly across the woven fabric. Another layer of flax woven fabric was added and the same procedure was repeated until the required number of fabric layers was stacked. Finally, a metallic roller was employed to compress and roll over the stacked laminate of woven fabric to ensure uniform distribution of the epoxy resin and the elimination of voids. The mould was closed and placed in the compression moulding machine under controlled pressure and room temperature for completing the curing process. The composite was released from the mould after 24 hours of curing. Thus-fabricated FFRE composites were subjected to the machining (milling) study to understand the effects of different input parameters on their behavior. Figure 2 shows the steps of the FFRE composite manufacturing procedure.

Milling test and selection of input parameters

A ceramic coated HSS end mill, with four flutes of different diameters, was used for milling the composite. The machining operation was executed in a vertical CNC machine. Initially, the FFRE composite specimen was securely mounted on the force dynamometer (Kistler), using a specially designed fixture. Milling was performed on the specimen, owing to which cutting forces were generated, these forces were sensed as an electrical signal by the force dynamometer. These signals were further digitized using a data acquisition system. Finally, these values were considered for assessing the milling efficiency of the FFRE composite.

Another important output factor to be evaluated is surface roughness; it was measured using a surface measurement device (TR-200). During the measurement, the probe was passed parallel to the channel axis and the average R_a value was recorded. Finally, the milled surface of the FFRE composite samples was examined using FESEM (Carl Zeiss Sigma-300, Schottky FEG) under different magnifications.

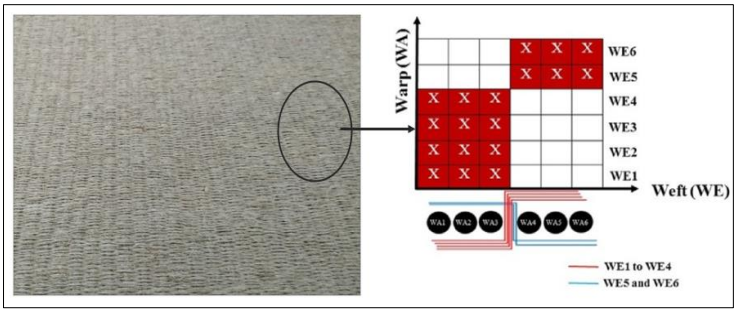

Figure 1: Woven flax fabric used as reinforcement[6]

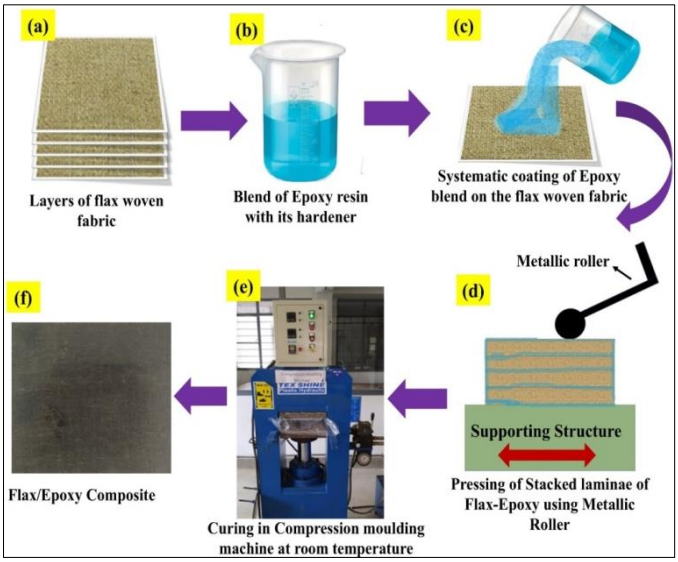

Figure 2: Preparation procedure followed for obtaining FFRE composites

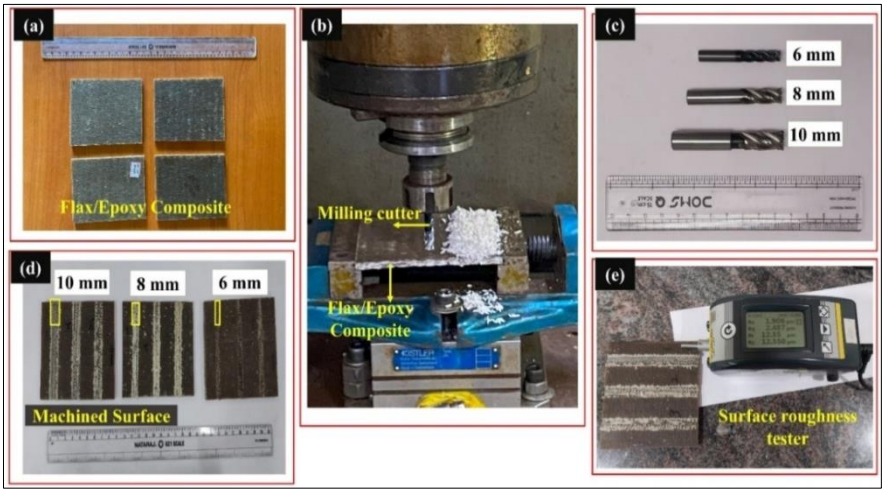

Figure 3: (a) FFRE composite, (b) Milling operation, (c) HSS-end mill cutters of various sizes, (d) Milled surfaces, and (e) Surface roughness measurement

Table 1
Input factors and their levels used for milling FFRE composite

Control factors	Levels			Units
	I	II	III	
Spindle speed (A)	900	1800	2700	rpm
Feed rate (B)	70	90	110	mm/min
End mill cutter (C)	6	8	10	mm

Three main parameters were selected as input factors, namely spindle speed (900, 1800, and 2700 rpm), feed rate (70, 90 and 110 mm/min), and size of the end mill cutters (6, 8, and 10 mm). The depth of cut was kept constant at 2 mm. The output characteristics considered for the evaluation were: cutting force and surface roughness (R_a). Hence, by understanding the suitable combination of input parameters, the cutting force required for machining the FFRE composite can be minimized and so its surface roughness value. Figure 3 depicts the overall process of milling the FFRE composite, starting from the milling operation to the measurement of the surface roughness value.

The milling process on the FFRE composites was performed for the given input conditions (Table 1). Experiments were designed as per Taguchi L_{27} orthogonal arrays. The obtained output responses obtained were cutting forces and surface roughness values, which were further studied to predict the machining performance using the ANN approach. The complete output milling responses obtained under different operating conditions are listed in Table 2.

Table 2
Experimental results for different input factors

Sl. No	Spindle speed (rpm)	Feed rate (mm/min)	Different sizes of end mill cutters (mm)	Cutting force (N)	Surface roughness (R_a)
1	900	70	6	19.321	6.251
2	900	70	8	26.786	11.020
3	900	70	10	40.745	16.859
4	900	90	6	21.345	8.184
5	900	90	8	32.781	12.783
6	900	90	10	43.031	18.883
7	900	110	6	22.425	10.338
8	900	110	8	39.669	15.551
9	900	110	10	45.143	19.111
10	1800	70	6	17.541	6.110
11	1800	70	8	24.581	8.975
12	1800	70	10	28.885	14.120
13	1800	90	6	20.045	7.448
14	1800	90	8	28.673	10.880
15	1800	90	10	32.334	15.557
16	1800	110	6	20.845	9.483
17	1800	110	8	35.579	13.297
18	1800	110	10	38.574	16.637
19	2700	70	6	16.666	5.393
20	2700	70	8	23.333	7.756
21	2700	70	10	26.765	12.920
22	2700	90	6	15.248	7.891
23	2700	90	8	26.879	8.888
24	2700	90	10	29.978	14.335
25	2700	110	6	14.852	9.158
26	2700	110	8	30.128	10.571
27	2700	110	10	34.786	15.587

Artificial Neural Networks (ANN)

ANN is a machine learning algorithm designed to predict solutions for complex problems. It is considered to mimic the structure and function of the human brain, and consists of three layers: input, hidden, and output. Each layer contains interconnected neurons that process and transfer information through weighted connections of the architecture. In the ANN architecture, data is fed into the input layer, passed to the hidden layers, and processed through weighted connections. The input values are multiplied by these weights, summed, and passed through an activation function before being sent to the successive layer. This process continues until the output layer predicts the final expected target. The ability of ANN to learn and identify patterns in input features makes it highly effective for modeling complex relationships between them. By training on experimental data, ANN can accurately predict targets, reducing the need for extensive physical experimentation trials.

ANN data processing procedure with employed topology and structure

In this study, ANN was employed to evaluate surface roughness (R_a) and cutting force based on experimental data. A feed-forward backpropagation neural network was used owing to its superior capability to handle complex nonlinear relationships. The network was created and optimized using MATLAB 2017, with input features (spindle speed, feed rate, end mill cutter size) and target data (surface roughness and cutting force) imported for training. The Levenberg-Marquardt algorithm was used for training the ANN architecture due to its fast learning ability. Parameters, such as the learning function, performance function (mean square error), and the number of neurons in the hidden layer, were optimized based on prior studies. The network was trained for a minimum of 100 epochs, with the mean square error (MSE) evaluated to assess model accuracy. If the MSE did not reach an acceptable value, the network weights were reinitialized, and training was repeated until an optimal model was developed. The final ANN model was developed based on the condition of achieving the minimum MSE value. The procedure to find out an optimal neural network model is indicated by the flow chart shown in Figure 4.

The feedforward neural network architecture was used in this research work. The spindle speed, feed rate, and tool diameter were the three input parameters for the proposed ANN architecture. These inputs were

processed through the hidden layer, where interconnected neurons apply weighted transformations before passing the information to the output layer. The network operates in a unidirectional manner, with no feedback loops, and aims to predict machining outputs, specifically cutting force and surface roughness, based on the relationships between input features. Figure 5(a, b) illustrates the single-output network architecture, where two separate ANN models were trained: one for cutting force and another for surface roughness (R_a). The backpropagation process iteratively adjusts the weights to minimize errors and improve prediction accuracy. This method allows the network to analyze each machining response independently, predicting the specific relationship of input features on each output. Using separate networks increases the computational cost because each model must be trained and validated individually.

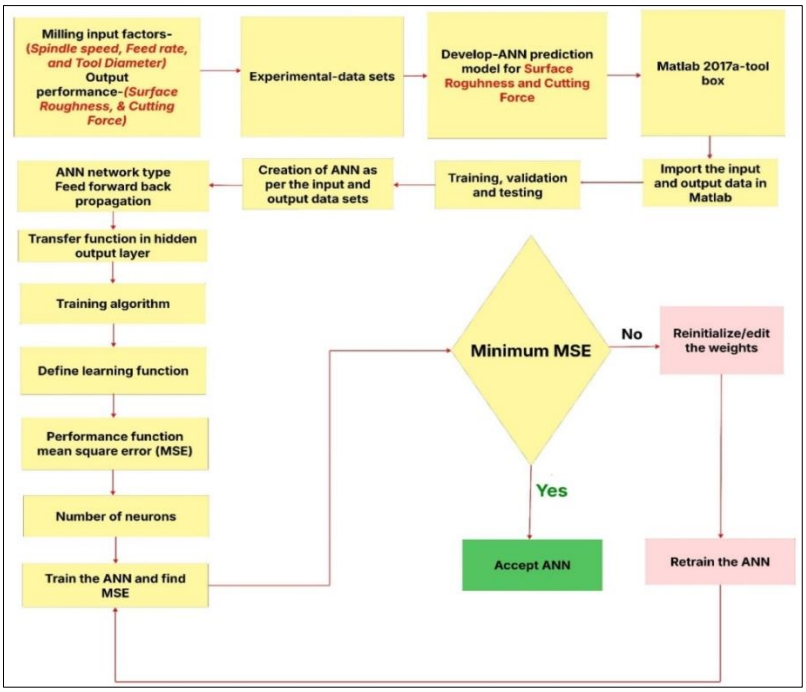

Figure 4: Procedure to reach the optimal neural network

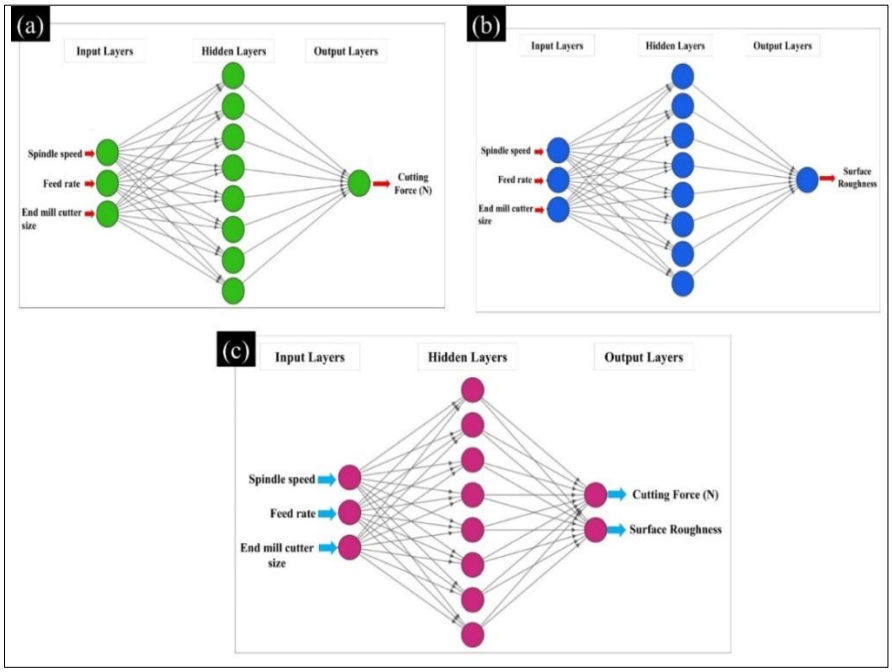

Figure 5: ANN with 3-n-1 topology for (a) cutting force, (b) surface roughness, and (c) ANN with 3-n-2 topology for dual responses

Figure 5(c) shows the dual-output network architecture, which predicts both cutting force and surface roughness in a single ANN architecture. This model used two output neurons for the respective machining responses. By processing input parameters together, the hidden layer can recognize relationships between machining factors, leading to more comprehensive predictions. The dual-output network architecture reduces training time and computational cost and improves efficiency by using a common hidden layer.

RESULTS AND DISCUSSION

Effect of input milling parameters on cutting force

From Figure 6, it can be noted that, during milling of FFRE composite specimens, cutting force increased with an increase in the feed rate. When the feed rate was raised, the tool may have not had enough time to cut the woven flax fibers used as reinforcement and a higher cutting force was required to overcome the flax fiber resistance. Experiments revealed that the milling cutter removed chips from the material by breaking the flax fibers, which may have been caused by a higher cutting force. At a higher feed rate, of 110 mm/min, higher cutting force (45.13 N) was generated as the cutting area engaged by the milling tool was larger, which directly increased friction and resistance. Similar findings were noted by Celik *et al.*[14] during milling of jute-epoxy composites. It is evident from Figure 6 that cutting force decreases with the increase in cutting speed during milling of the FFRE composites. This may be attributed to mainly friction between the cutting tool and FFRE composite specimen. During milling at higher cutting speed, the composite showed lower resistance to cutting force as the epoxy and the flax fiber tend to get softer at higher temperature. This significantly reduces the shear strength of the composite specimen, and demands only lower cutting force for milling.

As shown in Figure 7, as the cutting tool diameter increases, the cutting force required for material removal was also increased. Cutting force increased from 16.66 N to 45.13 N for different sizes of end mill cutters (6 mm, 8 mm and 10 mm). This significant increase in cutting force may be explained by the wider engagement area when using larger end mill cutters on the composite specimen, which required a higher amount of cutting force to remove material. However, cutting force during milling can be reduced by employing a smaller size end mill cutter, as it engages a lesser contact area on the specimen and may not demand higher cutting force to remove the material. Therefore, a smaller size end mill cutter was preferred. Though it demands a lower cutting force and provides higher surface finish, more passes were needed to cut the material and the risk of tool damage would be inevitable.

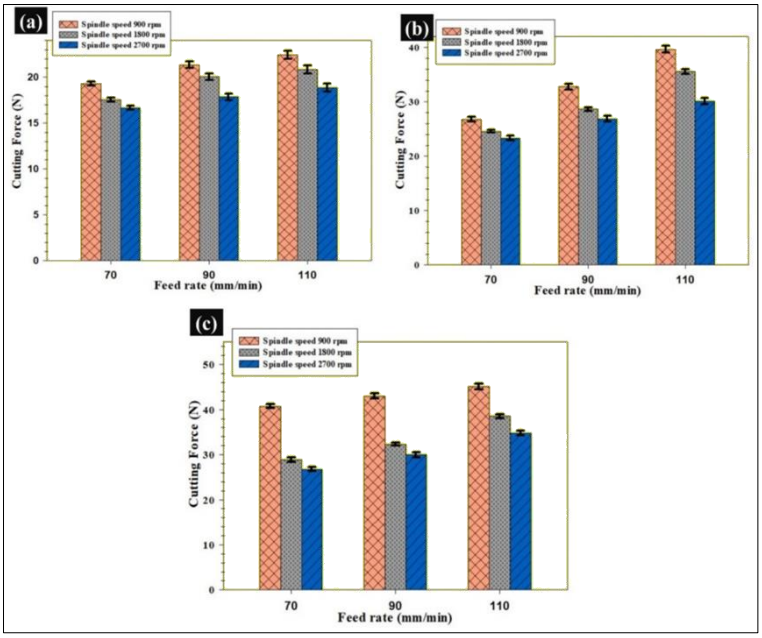

Figure 6: Variation of cutting force with respect to feed rate when milling using different end mill cutters: (a) 6 mm, (b) 8 mm and (c) 10 mm

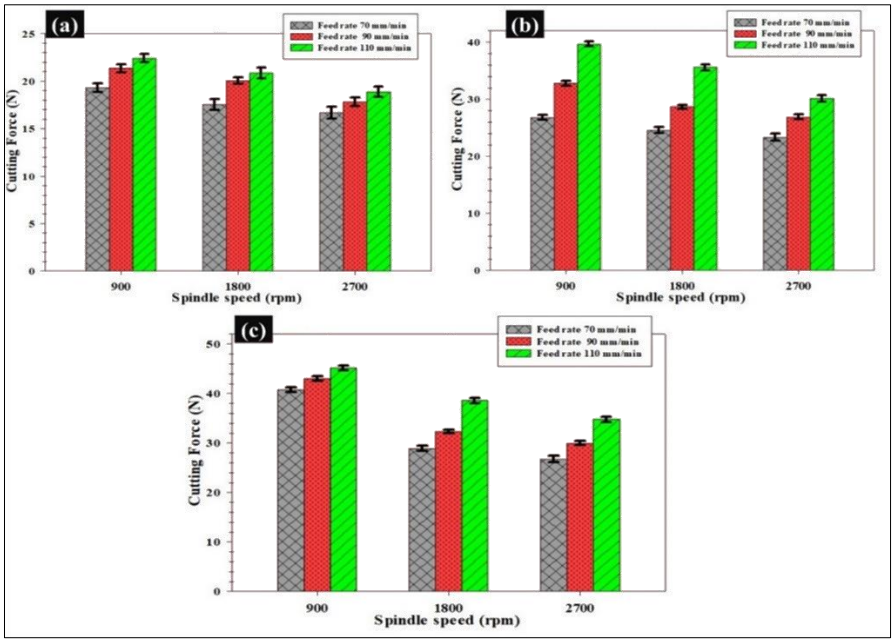

Figure 7: Variation of cutting force with respect to cutting speed when milling using different end mill cutters: (a) 6 mm, (b) 8 mm and (c) 10 mm

Effect of input milling parameters on surface roughness (R_a)

Surface roughness (R_a) is considered one of the essential parameters that determine the quality of the workpiece. Machining quality highly relies on the input parameters, namely cutting parameters and tool geometry. Thus, maintaining the R_a value as low as possible was key.[8] Figure 8 depicts the variation of surface roughness with respect to feed rate and spindle speed, when FFRE composites were milled with different sizes of end mill cutters. Surface roughness of the FFRE composite increases with the increase in feed rate, which may be attributed to the generation of a higher cutting force induced at a higher feed rate, paving the way for intense material removal. This causes major damage on the FFRE composite specimen, including fiber pull-out, surface unevenness, and matrix damage. However, in the case of a lower feed rate, the end mill cutter engages smoothly with the material, with a less intense cutting action, resulting in finer surface finish. Apart from that, increased feed rate causes unwanted vibration and tearing effect on the composite specimen, which may also deteriorate the surface finish, causing a rougher surface.

Surface roughness decreases with increasing cutting speed, as evident from Figure 9. Higher cutting speed was preferred, as it provides smoother surface finish than lower cutting speed. At higher cutting speed, the required cutting force for the removal of material was less and so the heat buildup zone was not significant, resulting in smoother cutting action, which eventually reduced fiber pull-out and matrix damage in the FFRE composite. While at lower cutting speed, on the contrary, the milling cutter engages roughly with the material, resulting in more tearing and uneven surface formation. Also, over time, a higher cutting speed may lead to higher cutting tool wear, which may deteriorate the surface finish of the FFRE composite material.

As the end mill diameter increases, the surface roughness of the FFRE composite material decreases. In this case, the end mill cutter of 10 mm yielded a finer surface, particularly when milling was performed at the spindle speed and feed rate of 2700 rpm and 70 mm/min, respectively. By employing a larger end mill cutter, better stability and more even distribution of the cutting force across a wider area can be accomplished, which results in smoother surface, indicated by lower surface roughness values. Also, a larger cutter reduces the vibration and deflection induced during the milling process, which eventually helps in reducing fiber pull-outs, and matrix damage. However, the reverse was true if a smaller end mill cutter was employed for milling the composite. A smaller cutter had higher cutting-edge engagement per revolution than larger ones, which results in intense material removal and a rougher surface.

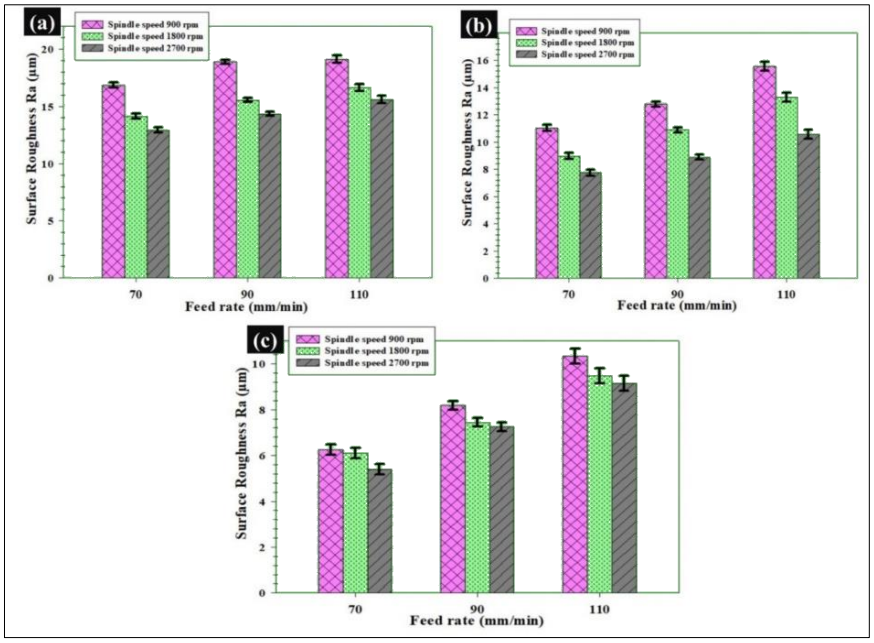

Figure 8: Variation of surface roughness with respect to feed rate when milling using different end mill cutters: (a) 6 mm, (b) 8 mm and (c) 10 mm

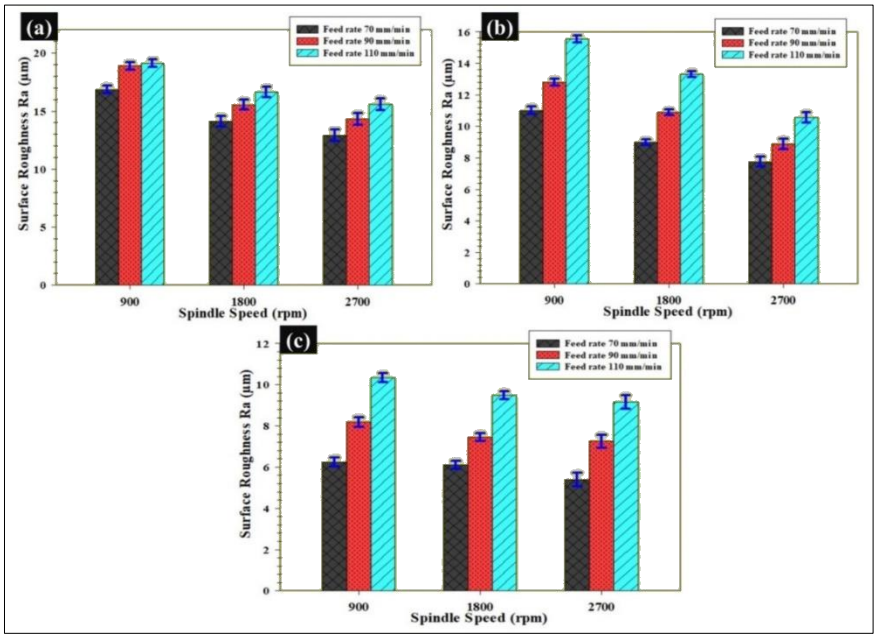

Figure 9: Variation of surface roughness with respect to spindle speed when milling using different end mill cutters: (a) 6 mm, (b) 8 mm and (c) 10 mm

ANN-based prediction of cutting force and surface roughness (R_a)

The ANN results are tabulated in Tables 3-5. Data shows the 3-5-4-1 architecture with Purelin-Purelin-Purelin activation exhibits the highest R^2 value – of 0.999437, with a MSE of 0.0000040 amongst the ANN models. This confirms that the Purelin-Purelin-Purelin transfer function helps predict cutting force with higher precision. Furthermore, in the ANN network, the 3-5-4-1 Logsig-Logsig-Purelin and the 3-5-4-1 Purelin-Purelin-Purelin transfer functions showed the least Mean Absolute Percentage Error (MAPE) values of 0.20% and 0.39%, respectively, suggesting the adopted networks were effective in predicting the cutting force.[24] In the case of the 3-7-6-1 architecture, the Logsig activation function in the hidden layers and following Purelin in the output layer may be significant in capturing nonlinear relationships data; whereas, in the 3-5-4-1 architecture, only Purelin

functions are effective, providing deeper networks with multiple layers. Similar observations were reported in previous studies.[24-26]

Similarly, the prediction of R^2 values and MSE for surface roughness was accomplished. The ANN 3-5-4-1 recorded the highest R^2 and MSE value of 0.99718 and 0.00001200, respectively. These predicted results imply that the developed ANN, with nine neurons in the hidden layers, with Purelin-Purelin-Purelin transfer function, predicts the surface roughness values with higher precision. Among the single hidden layer used, the 3-7-1 Transig-Purelin exhibited the lowest MAPE of 0.951%, while in multiple hidden layers, the 3-5-4-1 Purelin-Purelin-Purelin transfer function recorded 0.35%, suggesting these networks are effective in predicting the surface roughness values. ANN models with lower MAPE values are not only effective in predicting the experimental data sets with which they were trained, but also, have high precision in predicting unknown input parameters. Similar findings were reported in previous studies.[24-27]

Table 3
Summarized results for predicted cutting force using the 3-n-1 ANN model

Network structure	Transfer function			R^2 values				MSE
	Layer 1	Layer 2	Layer3	Training	Validation	Testing	All	Cutting force
3-4-1	Transig	Purelin		0.96454	0.98135	0.89714	0.96554	0.0010530
3-5-1				0.99476	0.99988	0.95204	0.98844	0.0003520
3-6-1				0.9954	0.79549	0.98865	0.97167	0.0068260
3-7-1				0.97632	0.47491	0.98411	0.94644	0.0459630
3-8-1				0.98731	0.96001	0.87608	0.97088	0.0018460
3-9-1				0.99285	0.95785	0.96397	0.96339	0.0001870
3-10-1				0.95253	0.75283	0.92499	0.92416	0.0062770
3-4-1	Logsig	Purelin		0.96642	0.87651	0.90831	0.91810	0.0010400
3-5-1				0.98739	0.84989	0.51646	0.93268	0.0334340
3-6-1				0.97936	0.94830	0.92408	0.95804	0.0003940
3-7-1				0.99031	0.98227	0.99393	0.98500	0.0000210
3-8-1				0.80964	0.99339	0.8606	0.78967	0.0063080
3-9-1				0.96071	0.84392	0.85984	0.92338	0.0022380
3-10-1				0.99507	0.99963	0.98401	0.98724	0.0000380
3-4-1	Purelin	Purelin		0.96170	0.98015	0.32815	0.93818	0.0750800
3-5-1				0.93684	0.98205	0.86992	0.94023	0.0016120
3-6-1				0.93267	0.96078	0.92117	0.94781	0.0002250
3-7-1				0.95315	0.98161	0.96750	0.94890	0.0001660
3-8-1				0.19504	0.92251	0.80494	0.07332	0.1366390
3-9-1				0.93418	0.95355	0.96650	0.93755	0.0001680
3-10-1				0.94570	0.93301	0.89303	0.94196	0.0004390
3-5-4-1	Transig	Transig	Purelin	1	0.99148	0.90224	0.95907	0.0010330
3-6-5-1				0.84823	0.77386	0.21131	0.80039	0.0673540
3-6-6-1				0.97075	0.97077	0.74872	0.95290	0.0088080
3-7-6-1				0.94487	0.83707	0.99189	0.94102	0.0032010
3-8-7-1				0.99986	0.72761	0.43306	0.90612	0.0466610
3-9-8-1				0.89796	0.94638	0.05817	0.782230	0.1288190
3-5-4-1	Transig	Purelin	Purelin	0.96658	0.92926	0.97403	0.95907	0.0002890
3-6-5-1				1	0.9011	0.71059	0.92153	0.0113070
3-6-6-1				0.99878	0.99323	0.77815	0.98415	0.0086060
3-7-6-1				0.95048	0.89025	0.92706	0.94102	0.0005250
3-8-7-1				0.87914	0.9995	0.99186	0.90612	0.0027530
3-9-8-1				0.97854	0.93369	0.99244	0.90628	0.0011910
3-5-4-1	Logsig	Logsig	Purelin	0.95295	1	1	0.95907	0.0004880
3-6-5-1				0.88479	1	0.99526	0.92153	0.0024030

3-6-6-1				0.99858	0.88723	0.99386	0.99358	0.0021950
3-7-6-1				0.97128	0.91331	0.74953	0.90067	0.0067090
3-8-7-1				0.99811	0.92326	0.99791	0.97604	0.0009330
3-9-8-1				0.99798	0.9623	0.72329	0.97278	0.0123030
3-5-4-1	Logsig	Logsig	Purelin	0.99692	0.98228	0.96968	0.98399	0.0000930
4-6-5-1				0.98399	0.99921	0.99301	0.99727	0.0000340
3-6-6-1				0.88998	0.99089	0.99552	0.99805	0.0020670
3-7-6-1				0.99358	0.99999	0.9927	0.98915	0.0000150
3-8-7-1				0.94775	0.98777	0.99792	0.97604	0.0003520
3-9-8-1	Purelin	Purelin	Purelin	0.99723	0.94759	0.92838	0.97917	0.0007170
3-5-4-1				0.99997	0.99842	0.99787	0.99437	0.0000040
3-6-5-1				0.97192	0.8188	0.95801	0.93436	0.0036460
3-6-6-1				0.99179	0.99954	0.99895	0.99358	0.0000110
3-7-6-1				0.98892	0.80425	0.98857	0.95739	0.0058430
3-8-7-1				0.96985	0.99734	0.9923	0.97604	0.0001280
3-9-8-1				0.92966	0.98909	0.31901	0.92766	0.0749790

Table 4
Summarized results for predicted surface roughness using the 3-n-1 ANN model

Network structure	Transfer function			R^2 values				MSE
	Layer 1	Layer 2	Layer3	Training	Validation	Testing	All	Surface roughness (R_a)
3-4-1	Transig	Purelin	—	0.99184	0.97473	0.99777	0.98991	0.00020000
3-5-1				0.96669	0.98734	0.98962	0.96583	0.00064000
3-6-1				0.99722	0.94794	0.99198	0.98445	0.00076000
3-7-1				1	0.99426	0.983	0.99525	0.00009000
3-8-1				0.95196	0.99591	0.94342	0.9364	0.00239000
3-9-1				0.98073	0.91692	0.99534	0.96535	0.00212000
3-10-1				0.99746	0.99607	0.98393	0.98879	0.00010000
3-4-1	Logsig	Purelin	—	0.9917	0.99971	0.9956	0.98991	0.00005000
3-5-1				0.96047	0.99984	0.907	0.96583	0.00284000
3-6-1				0.99633	0.96033	0.98667	0.99254	0.00046000
3-7-1				0.99383	1	1	0.99525	0.00002000
3-8-1				0.98782	0.97642	0.92267	0.98011	0.00177000
3-9-1				0.96418	0.98812	0.99564	0.96535	0.00066000
3-10-1				0.99103	0.99066	0.99967	0.998879	0.00004000
3-4-1	Purelin	Purelin	—	0.99072	0.99177	0.92609	0.98991	0.00143000
3-5-1				0.99744	0.99049	0.96118	0.9898	0.00043000
3-6-1				0.99627	0.96861	0.99911	0.9931	0.00026000
3-7-1				0.9991	0.99186	0.99501	0.99767	0.00002000
3-8-1				1	0.99305	0.99676	0.99815	0.00002000
3-9-1				0.99913	0.9994	0.96335	0.99014	0.00036000
3-10-1				0.99384	0.92722	0.97022	0.98879	0.00159000
3-5-4-1	Transig	Transig	Purelin	0.98797	0.97548	0.80111	0.97082	0.01029000
3-6-5-1				0.95703	0.89515	0.98981	0.9598	0.00364000
3-6-6-1				0.92025	0.87259	0.98098	0.93113	0.00692000
3-7-6-1				0.9997	0.97443	0.99947	0.98273	0.00024000
3-8-7-1				0.77524	0.62112	0.57003	0.68836	0.11902000
3-9-8-1				0.62828	0.94835	0.94733	0.69096	0.05978000
3-5-4-1	Transig	Purelin	Purelin	0.98429	0.99593	0.89449	0.97082	0.00306000
3-6-5-1				0.98483	0.9949	0.99173	0.98061	0.00018000
3-6-6-1				0.99778	0.92936	0.94385	0.97423	0.00220000
3-7-6-1				0.97868	0.96521	0.998	0.98273	0.00049000

3-8-7-1				0.99981	0.91676	0.35522	0.91972	0.10728000
3-9-8-1				0.99526	0.79734	0.84882	0.94315	0.01680000
3-5-4-1	Logsig	Logsig	Purelin	0.99961	0.99975	0.99265	0.99724	0.00002000
3-6-5-1				0.97523	0.99979	0.99608	0.98061	0.00025000
3-6-6-1				0.95334	0.99989	0.84244	0.97423	0.00692000
3-7-6-1				0.98097	0.9997	9.96727	0.98273	0.00017000
3-8-7-1				0.94858	0.45174	0.99991	0.91972	0.07742000
3-9-8-1				0.97299	0.97334	0.72733	0.94315	0.01976000
3-5-4-1	Logsig	Purelin	Purelin	1	0.94388	0.99322	0.99718	0.00080000
3-6-5-1				0.99688	0.99775	0.97043	0.9881	0.00026000
3-6-6-1				0.96225	0.99819	0.99992	0.97423	0.00052000
3-7-6-1				0.97275	0.99994	0.99977	0.98273	0.00026000
3-8-7-1				0.99999	0.79663	0.98239	0.96939	0.01065000
3-9-8-1				0.92886	0.99913	0.99876	0.94315	0.00207000
3-5-4-1	Purelin	Purelin	Purelin	0.99664	1	0.99968	0.99718	0.00001200
3-6-5-1				0.98764	0.98864	0.99627	0.9881	0.00011000
3-6-6-1				0.97915	0.86879	0.99956	0.97423	0.00458000
3-7-6-1				0.9806	0.99999	0.98026	0.98273	0.00027000
3-8-7-1				0.96099	0.99719	0.99959	0.96939	0.00062000
3-9-8-1				0.92007	0.98947	0.99998	0.94315	0.00243000

Table 5
Summarized results for predicted cutting force and surface roughness using 3-n-2 ANN model

Network structure	Transfer function			R^2 values				MSE	
	Layer 1	Layer 2	Layer 3	Training	Validation	Testing	All	Cutting force	Surface roughness (R_a)
3-4-2	Transig	Purelin		0.99668	0.98843	0.99501	0.99484	0.00170	0.00060
3-5-2				0.98466	0.96496	0.97190	0.97097	0.01330	0.00320
3-6-2				0.99086	0.99900	0.93631	0.98434	0.00570	0.00130
3-7-2				0.98454	0.96716	0.90884	0.97243	0.01530	0.00110
3-8-2				0.99968	0.99428	0.99329	0.99793	0.00050	0.00040
3-9-2				0.97592	0.99200	0.88712	0.94941	0.02350	0.00330
3-10-2				0.99723	0.98726	0.96095	0.99186	0.00300	0.00090
3-4-2	Logsig	Purelin		0.96587	0.98995	0.99204	0.96636	0.01520	0.00150
3-5-2				0.99322	0.98369	0.94803	0.98415	0.00570	0.00170
3-6-2				0.77250	0.99912	0.99030	0.98434	0.00570	0.00130
3-7-2				0.96507	0.99626	0.99610	0.97243	0.01530	0.00110
3-8-2				0.99833	0.99209	0.99980	0.99793	0.00050	0.00040
3-9-2				0.97316	0.99395	0.87012	0.94941	0.02350	0.00330
3-10-2				0.99121	0.98236	0.99810	0.99186	0.00300	0.00090
3-4-2	Purelin	Purelin		0.98099	0.99713	0.97483	0.98008	0.00810	0.00080
3-5-2				0.98357	0.98785	0.99615	0.98415	0.00570	0.00170
3-6-2				0.99260	0.99402	0.98754	0.99030	0.00320	0.00150
3-7-2				0.99219	0.97070	0.93105	0.97809	0.00900	0.00090
3-8-2				0.99749	0.99897	0.99989	0.99793	0.99950	0.99940
3-9-2				0.99862	0.92460	0.89630	0.97053	0.01290	0.00060
3-10-2				0.99272	0.99748	0.99748	0.99186	0.00300	0.00090
3-5-4-2	Transig	Transig	Purelin	0.99150	0.99480	0.93912	0.98169	0.00680	0.00170
3-6-5-2				0.95519	0.96717	0.98533	0.95695	0.03120	0.00300
3-6-6-2				0.93499	0.72926	0.92566	0.90680	0.04060	0.00620
3-7-6-2				0.99364	0.97394	0.92764	0.97551	0.00770	0.00350
3-8-7-2				0.98233	0.99495	0.90161	0.96917	0.01210	0.00250
3-9-8-2				0.85114	0.92465	0.86722	0.86779	0.05900	0.01050
3-5-4-2	Transig	Purelin	Purelin	0.98772	0.99589	0.95709	0.98169	0.00680	0.00170
3-6-5-2				0.99792	0.99216	0.97571	0.98985	0.00320	0.00170
3-6-6-2				0.86153	0.99458	0.99515	0.90680	0.04060	0.00620

3-7-6-2				0.97425	0.99227	0.95946	0.97551	0.00770	0.00350
3-8-7-2				0.97698	0.98987	0.90416	0.96917	0.01210	0.00250
3-9-8-2				0.96409	0.94554	0.96278	0.93924	0.02680	0.00540
3-5-4-2	Logsig	Logsig	Purelin	0.97156	0.99851	0.99688	0.98169	0.00680	0.00170
3-6-5-2				0.98988	0.99728	0.99114	0.98985	0.00320	0.00170
3-6-6-2				0.90298	0.97787	0.89699	0.90680	0.04060	0.00620
3-7-6-2				0.99037	0.98862	0.98899	0.98919	0.00280	0.00210
3-8-7-2				0.99297	0..98608	0.94893	0.98232	0.00560	0.00250
3-9-8-2				0.98418	0.91577	0.94460	0.95470	0.01640	0.00500
3-5-4-2	Logsig	Purelin	Purelin	0.99894	0.97528	0.97819	0.98883	0.00460	0.00070
3-6-5-2				0.98820	0.99606	0.99729	0.98985	0.00320	0.00170
3-6-6-2				0.99740	0.97585	0.98453	0.99219	0.00260	0.00110
3-7-6-2				0.94268	0.95253	0.83421	0.92121	0.03010	0.00630
3-8-7-2				0.97817	0.99279	0.99296	0.98232	0.00560	0.00250
3-9-8-2				0.94041	0.99967	0.99932	0.95470	0.01640	0.00500
3-5-4-2	Purelin	Purelin	Purelin	0.99759	0.98269	0.98876	0.99408	0.00250	0.00030
3-6-5-2				0.98859	0.99539	0.99362	0.98985	0.00320	0.00170
3-6-6-2				0.99217	0.99879	0.97514	0.99219	0.00260	0.00110
3-7-6-2				0.99940	0.98865	0.99086	0.99464	0.00200	0.00070
3-8-7-2				0.98068	0.98796	0.99288	0.98232	0.00560	0.00250
3-9-8-2				0.93341	0.99718	0.98111	0.95740	0.01640	0.00500

The 3-n-2 ANN models were further developed with different transfer functions to check their ability to predict combined output characteristics, namely cutting force and surface roughness values. The analysis of ANN results is listed in Table 5. The network 3-5-4-2 exhibited the highest R^2 value of 0.99408, with MSE of 0.00250, amongst the developed ANN models. In addition, the Purelin-Purelin-Purelin transfer function was found to be effective in predicting cutting force and surface roughness value closer to the target input data. The results demonstrated that MAPE for cutting force and surface roughness were less than those obtained with other 3-n-2 ANN models, with maximum R^2 value. Therefore, 3-5-4-2 with Purelin-Purelin-Purelin transfer function is a function that can be used to predict the output responses for unknown input parameters. Similar results were noted in previous studies.[24-27]

Figures 10 and 11 indicate the performance and regression plots for the 3-5-4-1 ANN model with Purelin-Purelin-Purelin transfer function. The performance plot with a negligible slope clearly shows its best fit had occurred due to the effective training. Hence, the trained ANN gives the output response with the least percentage of error and can be further utilized in predicting the output responses in future.[24,28]

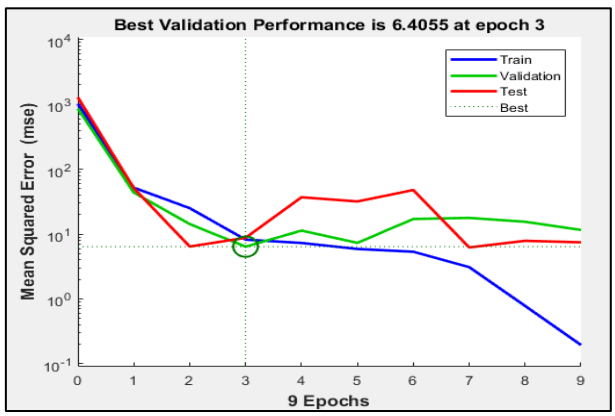

Figure 10: Performance plot for 3-5-4-1 ANN model with Purelin-Purelin-Purelin transfer function

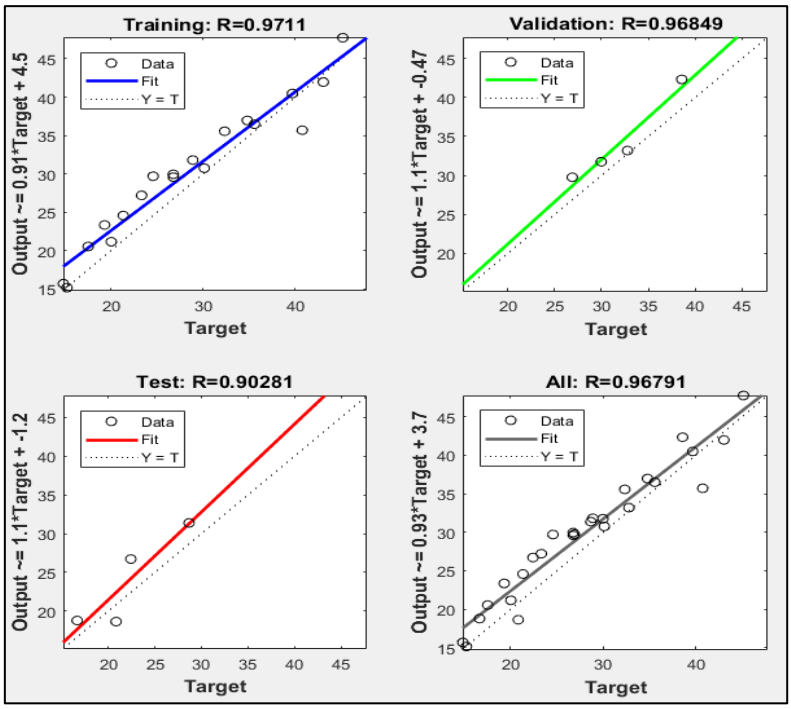

Figure 11: Regression plots for 3-5-4-1 ANN model with Purelin-Purelin-Purelin transfer function

Table 6
ANN (3-5-4-1) predicted cutting force for input data sets

Sl. No	Input data set			Predicted cutting force (N)	Predicted surface roughness (R_a)
	Spindle speed (rpm)	Feed rate (mm/min)	End mill cutter (mm)		
1	900	70	6	18.911	6.185
2	1800	70	6	18.123	6.249
3	1800	90	10	31.581	15.287
4	2700	90	8	26.514	9.218
5	2700	110	10	33.348	15.416

Table 7
Confirmation test results for cutting force with error percentage

Sl. No	Cutting force (N)		Error (%)
	Experimental	Predicted	
1	19.321	18.911	2.13
2	17.541	18.123	3.32
3	32.334	31.581	2.33
4	26.879	26.514	1.36
5	34.786	33.348	4.13

Table 8
Confirmation test results for surface roughness with error percentage

Sl. No	Surface roughness		Error (%)
	Experimental	Predicted	
1	6.251	6.185	1.06
2	6.110	6.249	2.27
3	15.557	15.287	1.74
4	8.888	9.218	3.71
5	15.587	15.416	1.10

Table 6 indicates the predicted cutting force and surface roughness of FFRE composites along with the input data set employed for the network. In the subsequent Tables 7-8 confirmatory test results for both responses are shown. These responses were obtained after performing the confirmation test and considered as the final step of the experimental work. Average values of three tests were reported. The difference between the actual values and the predicted values in terms of percentage error was computed and shown in Tables 7-8. The confirmation test shows that the error percentage between actual and predicted values is within the permissible limit of ±6%. Therefore, it can be concluded that the generated ANN, particularly the 3-4-5-1 model, can predict the cutting force and surface roughness with high accuracy.

FESEM analysis

The damage endured by FFRE composites during the milling process was observed using FESEM (Fig. 12). The cutting force plays a vital role in understanding the quality of the milled surface in FFRE composites. As discussed above, higher cutting force causes severe deformation and fiber pull-outs, deteriorating the mechanical properties of the composite. From Figure 12 (a), it is observed that fiber pull-outs are significant, considered as major damage that happens when the cutting force exceeds the bonding strength between flax fiber and matrix. Especially, when milling was performed using larger size cutter, flax fiber was more vulnerable to detaching from the epoxy matrix, leading to exposed fiber and cavities on the machined surface of the FFRE composite, as indicated in Figure 12 (a, b). This generally weakens the composite structure because of increased porosity. Furthermore, Figure12 (b) shows delaminated layers of the composites, which may be associated to higher cutting force, as it is the dominant factor in separating the flax/epoxy laminates, and eventually deteriorating the mechanical integrity of the composite material.

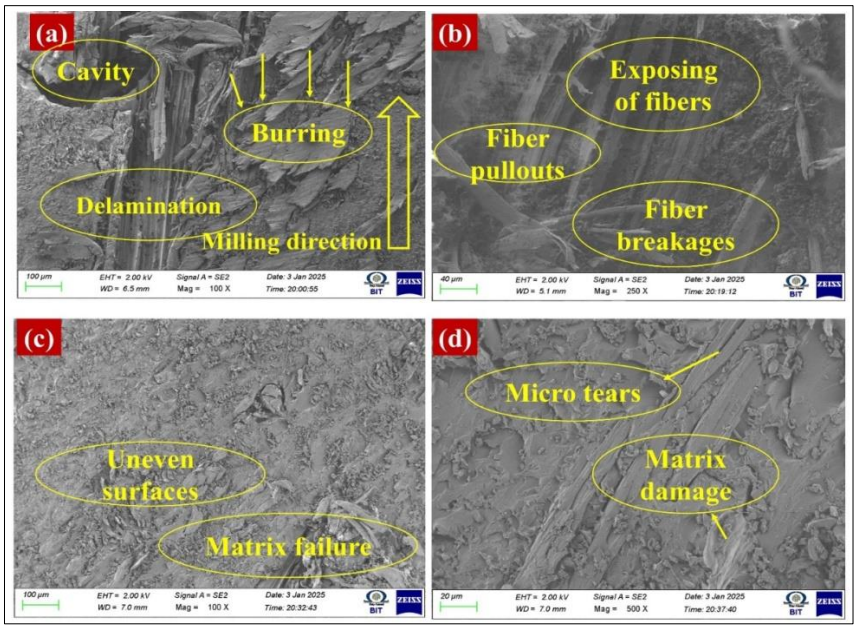

Figure 12: FESEM images of the machined surface of FFRE composites milled under the test conditions: (a, b) feed rate of 70 mm/min, end mill cutter size of 10 mm, spindle speed of 900 rpm; (c, d) feed rate of 70 mm/min, end mill cutter size of 6 mm and spindle speed of 900 rpm

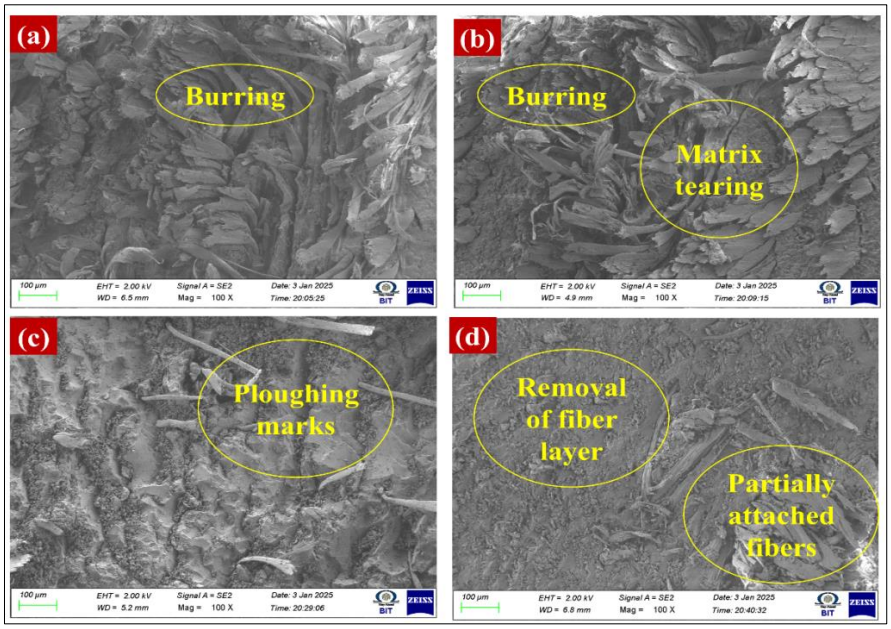

Figure 13: FESEM images of the machined surface of FFRE composites milled under the test conditions: (a, b) feed rate of 110 mm/min, end mill cutter size of 6 mm, spindle speed of 900 rpm; (c, d) feed rate of 110 mm/min, end mill cutter size of 10 mm and spindle speed of 900 rpm

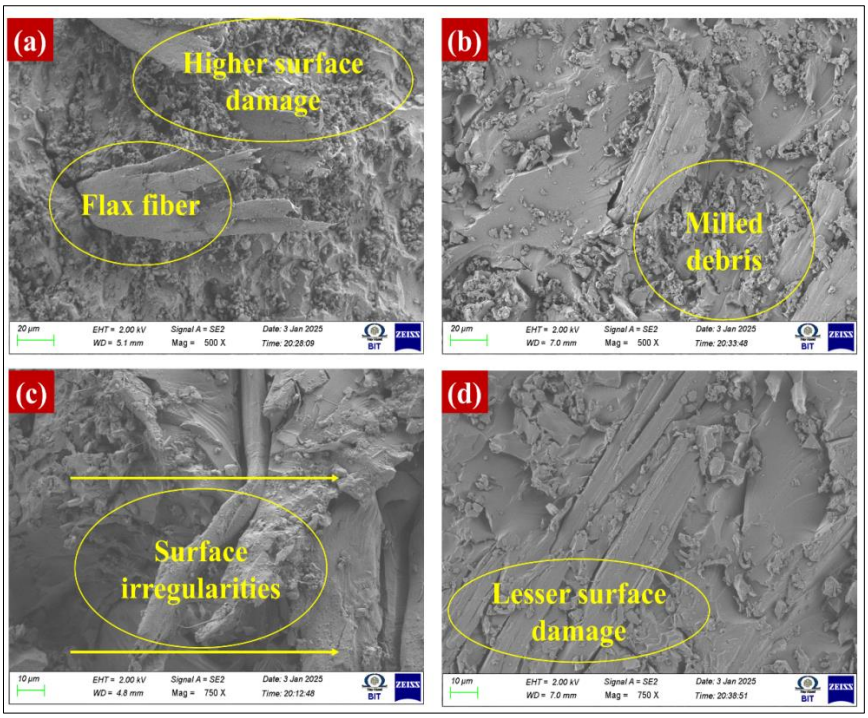

Figure 14: FESEM images of the machined surface of FFRE composites milled under the test conditions: (a, b) feed rate of 70 mm/min, end mill cutter size of 6 mm, spindle speed of 2700 rpm; (c, d) feed rate of 110 mm/min, end mill cutter size of 10 mm and spindle speed of 2700 rpm

On the other hand, surface roughness plays a key role in determining the quality of the milled surface. It is noted in the FESEM images that poor surface finish is associated with increased fiber breakages and micro-tear. In Figure13, broken flax fiber and micro-tear along the machining patch is clearly seen. This may happen because of the higher feed rate and smaller size of the end mill cutter. Figure13 further discloses the partially removed flax fiber, remaining still attached to the matrix, termed as “burring”. This fiber burring effect often leads to surface irregularities and may result in higher surface roughness values. However, delamination, burring, micro-tear, fiber breakage, and fiber pullout were significantly reduced, as indicated in the micrographs (Fig. 14), when the composite was

milled under the optimized test conditions, while unevenness in the surface was inevitable. For achieving better surface quality of the milled surface, a larger size end mill cutter operated at higher spindle speed with lower feed rate would be recommendable.

CONCLUSION

The conclusions drawn based on the experimental results and analysis are presented below.

One of the main responses considered in this study was cutting force. This cutting force increased with an increase in the feed rate. Higher cutting force was generated when the FFRE composite was milled with a feed rate of 110 mm/min using the 10 mm HSS end mill cutter at the cutting speed of 900 rpm.

The lower the cutting force generated during milling, the better the surface finish of the composites. In this study, a lower cutting force of 14.85N was obtained under optimal conditions when the FFRE composite was milled at the cutting speed of 2700 rpm, using a small size (6 mm) end mill cutter, with a feed rate of 110 mm/min. At higher cutting speed, the friction between the tool and the material surface plays an important role. Especially, matrix softening due to higher temperature at the tool-work interface significantly reduces the fiber resistance to cutting. Thus, a lower cutting force was produced.

Surface roughness (R_a) of the composite increased with an increase in the feed rate. This was caused by intense material removal at higher feed rate. The highest R_a value (19.11 μm) was found when machining was performed at a cutting speed of 900 rpm, feed rate of 110 mm/min, using a 10 mm end mill cutter. Such input conditions are not recommended for achieving a high-quality machining surface in FFRE composites.

FESEM images clearly presented the fiber breakage and exposure, micro-tear, matrix cavities and layer delamination, which were predominant when the composites were milled at a higher feed rate and lower cutting speed, particularly using smaller end mill cutters.

Amongst the ANN models trained, for single output response, the 3-5-4-1 Purelin-Purelin-Purelin transfer functions were found to be effective in predicting both cutting force and surface roughness, with R^2 values of 0.99437 and 0.99718, respectively. For dual output functions, the 3-5-4-2 Purelin-Purelin-Purelin transfer functions achieved an R^2 value of 0.99408. Furthermore, the validation of the ANN model was performed successfully. Predicted results were found in close agreement with the experimental results, with deviation within the acceptable limits. Thus, the trained neural networks were highly reliable in predicting the test results.

REFERENCES

[1] M. Alarifi, *J. Nat. Fibers*, **20** (2023), https://doi.org/10.1080/15440478.2022.2154304

[2] M. Kabir, H. Wang, K. Lau and F. Cardona, *Compos. Part B Eng.*, **43**, 2883 (2012), https://doi.org/10.1016/j.compositesb.2012.04.053

[3] L. Yan, N. Chouw and K. Jayaraman, *Compos. Part B Eng.*, **56**, 296 (2014), https://doi.org/10.1016/j.compositesb.2013.08.014.

[4] V. K. Shettahalli Mantaiah, *J. Nat. Fibers*, **19**, 12415 (2022), https://doi.org/10.1080/15440478.2022.2060404

[5] S. V. Kumar and H. Singh, *Indian J. Fibre Text. Res.*, **48**, 326 (2023), https://doi.org/10.56042/ijftr.v48i3.6057

[6] V. K. Shettahalli Mantaiah, S. K. Kallippatti Lakshmanan and S. Kaliappagounder, *J. Nat. Fibers*, **19**, 10367 (2022), https://doi.org/10.1080/15440478.2021.1993504

[7] S. V. Kumar, K. S. Kumar and H. S. Jailani, *Mater. Res. Express*, **7**, 085302 (2020), https://doi.org/10.1088/2053-1591/abaea5

[8] E. Sakthivelmurugan, G. Senthil Kumar and S. Vinu Kumar, *J. Braz. Soc. Mech. Sci. Eng.*, **45**, 400 (2023), https://doi.org/10.1007/s40430-023-04339-y

[9] S. M. V. Kumar, R. Jeyakumar, N. Manikandaprabhu and C. Sasikumar, *Cellulose Chem. Technol.*, **58**, 833 (2024), https://doi.org/10.35812/CelluloseChemTechnol.2024.58.74

[10] D. E. Raja, S. P. Selvan, P. Prabhuraj and T. Sonar, *Adv. Mater. Sci. Eng.*, **2022**, 4614105 (2022), https://doi.org/10.1155/2022/4614105

[11] T. Valarmathi, K. Palanikumar, S. Sekar and B. Latha, *Mater. Manuf. Process.*, **35**, 469 (2020), https://doi.org/10.1080/10426914.2020.1711931

[12] S. M. Vinu Kumar, N. Manikandaprabu, N. Babu and C. Sasikumar, *Cellulose Chem. Technol.*, **58**, 101 (2024), https://doi.org/10.35812/CelluloseChemTechnol.2024.58.10

[13] S. Jayabal, U. Natarajan and U. Sekar, *Int. J. Adv. Manuf. Technol.*, **55**, 263 (2011), https://doi.org/10.1007/s00170-010-3030-7
[14] Y. H. Çelik, E. Kilickap and A. İ. Kilickap, *J. Compos. Mater.*, **53**, 3127 (2019), https://doi.org/10.1177/0021998319826 37
[15] R. Vinayagamoorthy and N. Rajeswari, *Int. J. Compos. Mater. Manuf.*, **2**, 15 (2012)
[16] G. D. Babu, K. S. Babu and B. U. M. Gowd, *J. Adv. Mech. Eng.*, **1**, 1 (2013), https://doi.org/10.1177/09544089221126087
[17] A. L. Kumar and M. Prakash, *Polym. Polym. Compos.*, **29**, S178 (2021), https://doi.org/10.1177/0967391121991289
[18] F. Chegdani, S. Mezghani and M. El Mansori, *Wear*, **332**, 772 (2015), https://doi.org/10.1016/j.wear.2014.12.039
[19] M. Slamani, H. Chafai and J. Chatelain, *Proc. Inst. Mech. Eng. Part E J. Process Mech. Eng.*, **238**, 1537 (2024), https://doi.org/10.1177/09544089221126087
[20] S. Ragunath, M. L. Rathod and K. Saravanan, *J. Nanomater.*, **2023**, 9485769 (2023), https://doi.org/10.1155/2023/9485769
[21] P. P. Prasanthi, V. V. Madhav and C. S. Chaitanya, *Adv. Mater. Process. Technol.*, **10**, 1943 (2024), https://doi.org/10.1080/2374068X.2023.2204774
[22] S. Ghafarizadeh, G. Lebrun and J.-F. Chatelain, *J. Compos. Mater.*, **50**, 1059 (2016), https://doi.org/10.1177/0021998315587131
[23] H. Wang, J. Sun and J. Li, *Mater. Technol.*, **30**, A46 (2015), https://doi.org/10.1179/1753555715Y.0000000002
[24] A. V. Borgaonkar and S. Ismail, *Proc. Inst. Mech. Eng. Part C J. Mech. Eng. Sci.*, **236**, 6835 (2022), https://doi.org/10.1177/09544062211065995
[25] A. K. F. Hassan and S. Mohammed, *Univ. J. Mech. Eng.*, **4**, 39 (2016), https://doi.org/10.13189/ujme.2016.040204
[26] P. S. Kumar and K. Manisekar, *Indian J. Eng. Mater. Sci.*, **21**, 657 (2014)
[27] Z. Zhao, H. Xin, Y. Ren and X. Guo, in *Procs. 2010 International Conference on Measuring Technology and Mechatronics Automation* (*ICMTMA*), 2010, vol. 1, pp. 590–593, https://doi.org/10.1109/ICMTMA.2010.492
[28] J. Zhu, Y. Shi, X. Feng, H. Wang and X. Lu, *Mater. Des.*, **30**, 1042 (2009), https://doi.org/10.1016/j.matdes.2008.06.045